PHOTON
Journal of Natural Sciences and Technology
p-ISSN: 2087-393X | e-ISSN: 2579-5953
http://ejurnal.umri.ac.id/index.php/photon

Synthesis and Molecular Docking Study of 2-(3-(3-methoxyphenyl) -6-oxopyridazin-1(6H)-yl)acetohydrazide as Potential Anticancer Agent for Breast Cancer

Putri Mar Atus Shalihah, Winda Permata Zulmy, Rudi Hendra, Jasril*

Department of Chemistry, Faculty of Mathematics and Natural Sciences, Universitas Riau, Indonesia

Received 19 May 2025 | Accepted 21 July 2025 | Published 30 November 2025
DOI: https://doi.org/10.37859/jp.v16i1.9167

Keywords:

Pyridazinone;
Acetohydrazide;
Breast cancer;
Estrogen alpha

Abstract. Pyridazinones are a class of heterocyclic compounds with broad biological activities, one of which is as an anticancer. This study synthesized N-acetohydrazide substituted pyridazinone derivatives and evaluated their potential as breast cancer therapy through molecular docking studies. The target compound, 2-(3-(3-methoxyphenyl)-6-oxopyridazine-1(6H)-yl)acetohydrazide**(3)**, was synthesized through three reaction steps: condensation to form the pyridqzinone core, functionalization of ethyl chloroacetate at the nitrogen position, and substitution of the ethoxy group with hydrazine hydrate. The yield obtained was 48.14%. The purity of the synthesized compound was confirmed through melting point determination and high-performance liquid chromatohraphy (HPLC) analysis, which showed a single dominant peak. Structural elucidation using Fourier-transform infrared (FTIR), mass spectrometry (MS), proton nuclear magnetic resonance (^{1}H-NMR), and carbon-13 nuclear magnetic resonance (^{13}C-NMR) verified the expected structure. Molecular tethering studies against tyrosine kinase (PDB ID: 3ERT) showed that compound **(3)** has a binding free energy of -7.93 kcal/mol, with two hydrogen bonds formed with residues Glu353 and Leu387. These results indicate that compound **(3)** has not shown better inhibitory activity than tamoxifen. Nonetheless, this compound fulfils good physicochemical characteristics based on Lipinski's rule, so it remains promising for further development

*Corresponding author.
E-mail address: jasril.k@lecturer.unri.ac.id

1. Introduction

Breast cancer is one type of cancer with a high incidence of cases in the world, especially in women. According to Arnold et al. (2022) in the last five years, approximately 7.8 million women were diagnosed with breast cancer. In Indonesia, it was recorded that the incidence of breast cancer reached 65,858 cases (Gondhowiardjo et al., 2021; Yuliastuti et al., 2023). The high number of incidence indicates that breast

cancer is still a global health problem that requires special attention in an effort to provide more effective and safe therapy. The World Health Organization (WHO) has launched the Global Cancer Initiative (GBCI) programme with the aim of reducing breast cancer mortality by 2.5% per year and preventing 2.5 million breast cancer deaths worldwide by 2040. The programme focuses on early detection, timely diagnosis and treatment as its key pillars (Ong et al., 2024).

Currently various breast cancer treatment methods are available, surgery combined with chemotherapy and radiotherapy is the standard treatment in breast cancer (Moo et al., 2018). Estrogen receptor alpha (ER-α) is considered to be the receptor most involved in breast cancer cell development. Therefore, this receptor is an important target in breast cancer therapy (Clusan et al., 2023). One of the drugs used for breast cancer therapy currently is tamoxifen (Oskoueian et al., 2018), which acts by attaching to estrogen receptors in the endoplasmic reticulum, thereby inhibiting the activation of estrogen expression in breast cells (Chesney et al., 2017). Although they work well, long-term use of these drugs may develop resistance that reduces the performance and effectiveness of the drug (Mirzaei et al., 2022). This then encourages the need for research into the development of new anticancer candidates that work more specifically.

One approach to breast cancer drug development is the exploration of bioactive compounds from natural and synthetic sources. Pyridazinones are a class of heterocyclic compounds with two nitrogen atoms, which makes these compounds have a broad spectrum of biological activity (Qin et al., 2020). So o far, pyridazinone-derived compounds have been investigated and showed good inhibitory activity against Vascular Endothelial Growth Factor Receptor 2 (VEGFR-2) (El-Nagar et al., 2024) and Epidermal Growth Factor Receptor (EGFR) (Merde et al., 2023) which is responsible for the growth of various cancer cells. Therefore, in this study, the activity of pyridazinone derivatives containing acetohydrazide substituents as ER-α inhibitors was studied through molecular docking studies, with the aim of finding new breast anticancer drug candidates. In addition, the pharmacokinetics and ADMET profiles of the target compounds were also studied.

2. The Methods

2.1. Materials and Tools

Materials used include 3-methoxyacetophenone (Merck), glyoxylic acid (Merck), hydrazine monohydrate (Merck), ethylchloroacetate (Merck), potassium carbonate (Merck), glacial acetic acid (Merck), dimethylformamide (Merck), ethanol p.a (Merck), methanol p.a (Merck), NaOH 6 N, silica gel GF 254 TLC plate (Merck), universal pH indicator (Merck), distilled water and several technical solvents such as ethyl acetate, methanol, and n-hexane that have been distilled.

Tools used in this study include analytical balance (NEWTECH), magnetic stirrer, ACE pressure tube, hotplate (BOECO Germany), oven, Fisher John melting point determinant (SMP 11-Stuart), UV lamp (Camag® 254 and 365 nm), HPLC (UFLC Prominance Shimadzu LC Solution, SPD 20AD UV detector), FTIR spectrophotometer (FTIR Shimadzu, IR Prestige-21), NMR spectrophotometer (Agilent 500 MHz with DD2 console system), mass spectrophotometer (Water LCT premier XE positive mode), and glassware commonly used in Chemistry Laboratory FMIPA Riau University. Equipment for molecular docking assays included an LG Intel® CoreTM i7-8700 computer, 3.20 GHz CPU with 8.0 GB RAM, equipped with ChemDraw Professional 15.0 and MOE 2022.02 (Molecular Operating Environment, Chemical Computing Group, Tokyo, Japan). All programmes were run on a 64 bit operating system, Windows 10 Pro

2.2. Synthesis of compound 6-(3-methoxyphenyl)pyridazine-3(2H-one) (1)

A total of 3 mmol of 3-methoxyacetophenone and 3 mmol of glyoxylic acid were put into a monowave tube, then added with 3 mL of glacial acetic acid. The mixture was reacted using a monowave at 120˚C for 4 hours. Then 3 mmol of hydrazine hydrate was added and the reaction was continued for 3 hours. Reaction control was carried out using TLC every one hour. The mixture was then neutralised with 6 N NaOH to form a precipitate. The mixture was placed in a freezer for 24 hours. The precipitate was filtered and recrystallised using hot ethanol and obtained as compound **(1).**

Molecular formula $C_{11}H_{10}N_2O_2$, brown solid (75.47% yield), melting point 180-182˚C. FT-IR spectrum (KBr) Ū (cm^{-1}): 3152 (N-H amine), 3073 and 1489 (C-H sp^2), 1678 (C=O), 1594 (C=N), 1284 (C-N).

2.3. Synthesis of compound ethyl-2-(3-(3-meyhoxyphenyl)-6-oxopyridazine-1(6H)-yl)acetate (2)

A total of 1 mmol of compound **(1)** was mixed with 1.5 mmol ethylchloroacetate and 2 mmol potassium carbonate in 5 mL dimethylformamide into an Ace pressure tube. The mixture was reacted by stirring method for 3 hours at room temperature. Reaction control was carried out once an hour using TLC. The mixture was then poured into a container filled with DM ice and put into the freezer for 24 hours. The precipitate was separated by filtering and obtained as compound **(2)**.

Molecular formula $C_{15}H_{16}N_2O_4$, yellow solid (88.44% yield), melting point 68-69˚C. FT-IR spectrum (KBr) Ū (cm-1): 3081 and 1419 (C-H sp2), 1741 (C=O), 1600 (C=N), 1299 (C-O), 1162 (O=C-O-C acetate).

2.4. Synthesis of compound 2-(3-(3-methoxyphenyl)-6-oxopyridazine-1(6H)-yl)acetohydrazide (3)

A total of 1 mmol of compound **(2)** and 3 mL of hydrazine hydrate were put into an Ace pressure tube. Then 25 mL of methanol was added. The mixture was reacted by stirring method for 3 hours at room temperature. Reaction control was carried out once an hour using TLC. The mixture was then poured into a container filled with DM ice and put into the freezer for 24 hours. The precipitate formed was then filtered, dried and obtained as compound **(3).**

Molecular formula $C_{13}H_{14}N_4O_3$, white solid (48.14% yield). m.p 160-162˚C. FT-IR spectrum (KBr) Ū (cm^{-1}): 3326 (N-H), 3057 (C-H sp^2), 1666 (C=O), 1585 (C=N), 1299 (C-O). 1H-NMR (500 MHz, CDCl3) δ (ppm): 8.0148-7.9954 (d, J= 9.7 Hz, 1H), 7.0784-7.0589 (d, J=9.7 Hz, 1H), 7.02-7.00 (d, J= 7.6 Hz ,1H), 7.4181 (s, 2H), 7.3928-7.3604 (t, J= 8.05, 1H), 4.8817 (s, 2H), 3.8429 (s, 3H). HRMS (ESI): m/z 275.1148 [M + H]+ (calcd. for C1 C13H14N4O3: 274.28).

2.5. Purity analysis and characterisation

Purity analysis of the synthesised compounds was carried out by melting point measurement and High Performance Liquid Chromatograpgy (HPLC) analysis. The structure of the target compound **(3)** was characterised by spectroscopic analysis including Fourier Transform Infra Red (FT-IR), mass spectroscopy (MS), and Nuclear Magnetic Resonance (^{1}H and ^{13}C NMR).

2.6. Molecular docking test

The molecular structure of compound **(3)** and Tamoxifen as positive control were drawn using ChemDraw Professional 15.0. Afterwards, the 3D molecular structures were refined using the Molecular Operating Environment (MOE) 2022.0901 software package from the Chemical Computing Group, utilizing the MMFF94x force field and a gradient of 0.0001 utilizing all these refined molecular structures, a ligand database in *.mdb format was then created.

The molecular structure of protein tyrosine kinase was obtained from Protein Data Bank with PDB ID 3ERT (https://www.rcsb.org/). Protein crystal structure preparation can be used MOE 2022.0901 software from Chemical Computing Group and Discovery Studio Visualizer (DSV) from Biovia

Software package. Protein energy minimization was performed using the CHARMM27 force field, with an RMS gradient of 0.01 kcal/mol applied throughout the process. As a result of this energy minimization, the protein structure was then used as a receptor in the analysis.

Moleculer docking was conducted in an oriented manner by first identifyng the active site of the protein. The site finder tool was employed to localize the active site, and it was designated as a dummy atom. Subsequently, the posture and refinement parameters were set to 50 and 10, respectively, and the placement of the triangle was determined. With these preparations complete, docking could be promptly initiated.

2.7. ADMET Profiles

ADME (Absorption, Distribution, Metabolism, and Excretion) and toxicity profile analyses were performed using the ADMETlab 2.0 online server (https://admetmesh.scbdd.com/service/evaluation/index) as performed by Frimayanti et al., 2025. The first step, the SMILES code of the target compound structure was generated using the SwissADME website ((http://www.swissadme.ch/index.php). The code is then copied and placed on the ADMETlab website after clicking Run, then a complete ADMET profile will appear along with Lipinski's rule of five from the analysed target compound.

3. Result and Discussion

3.1. Chemistry

In this study, the synthesis of the target compound was carried out through three reaction steps. The first step was synthesized of 6-(3-methoxyphenyl)pyridazine-3(2H)-one **(1)**. The second step is the synthesis of ethyl-2-(3-(3-methoxyphenyl)-6-oxopyridazin-1(6H)-yl)acetate **(2)**. The third step is the synthesis of 2-(3-(3-methoxyphenyl)-6-oxopyridazin-1(6H)-yl)acetohydrazide **(3)**. The synthesis route of the target compound can be seen in Figure 1.

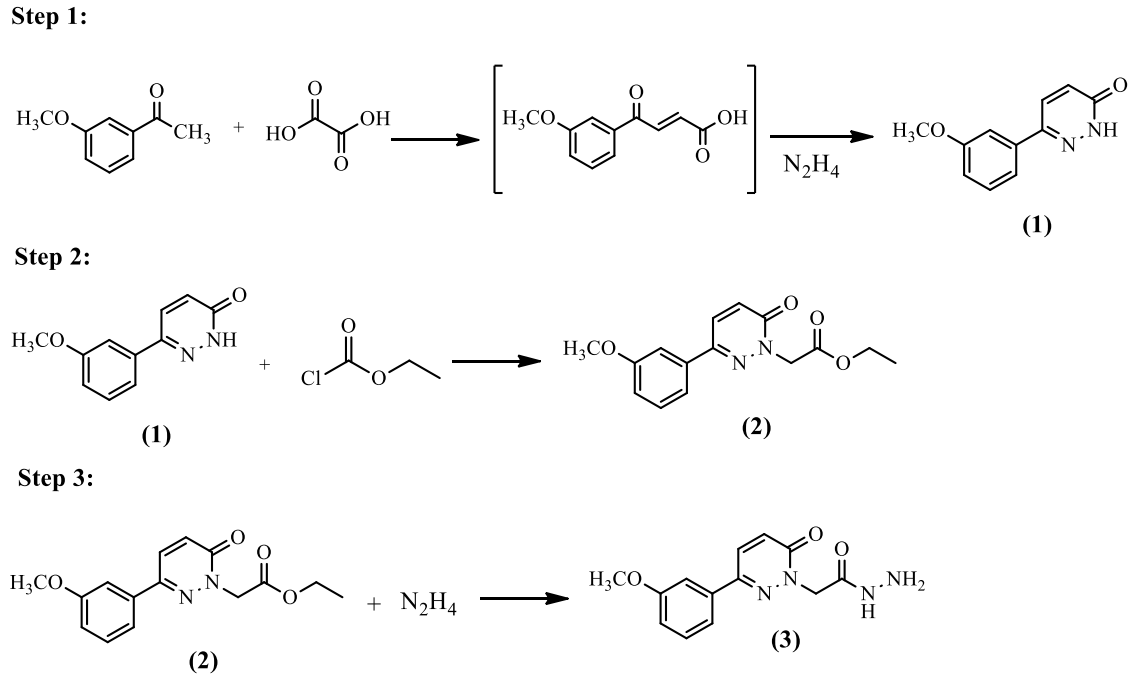

Figure 1. Design concept for synthesis target compound **(3).**

The first stage of synthesis of the target compound started with the formation of pyridazinone compound through aldol condensation reaction between acetophenone and glyoxylic acid using one-

pot method (Xu et al., 2006). This reaction involves the formation of an enol from acetophenone and reaction with protonated glyoxylic acid, resulting in a βihydroxy ketone compound that then dehydrates to a conjugated enone, oxobutenoic acid (Casale et al., 2007). This compound then reacts with hydrazine hydrate under acidic conditions through a cyclisation reaction to form compound **(1)**. The formation of the product is indicated by a change in colour to dark brown and the appearance of a new stain on TLC. The reaction was neutralised by the addition of 6N NaOH, then the mixture was kept in a freezer for 24 hours to precipitate the product. The product was obtained as compound **(1)** in the form of brown solid with 75.47% yield.

The second step was the substitution of compound (1) with ethylchloroacetate at the N position to form ethyl-2-(3-(3-methoxy phenyl)-6-oxopyridazine1(6H)-yl)acetate compound **(2)**. This reaction was catalysed by K_2CO_3 in dimethylformamide (DMF) solvent with stirring method at room temperature. K_2CO_3 is a heterogeneous catalyst that is alkaline, where O- will take hydrogen atoms from the N-H group in compound (1). This can increase the nucleophilic nature of nitrogen atoms, so that nitrogen will attack the carbon in ethyl chloroacetate and followed by the release of Cl groups. This reaction is sensitive to water so the use of DMF solvent will not interfere with the effectiveness of the reaction. Compound **(2)** was obtained as a yellow coloured solid with a yield of 88.44%.

The third stage is the substitution of compound **(2)** with hydrazine hydrate in methanol solvent to form compound **(3)**. The nitrogen in hydrazine acts as a nucleophile that attacks the carbon cation of compound **(2)** so that the phi bond on the carbonyl will move to the O atom and the intermediate product is formed. Furthermore, the release of ethoxy group occurs and acetohydrazide group is formed. Compound **(3)** was obtained as a white solid with a yield of 48.14%.

The compound **(3)** were characterization on the basis of IR, MS, ^{1}H NMR and ^{13}C NMR spectral data. IR spectrum showed the characteristics band at 3326 cm^{-1} region which indicate N-H vibrations (Meister et al., 2017), peak 2836 cm^{-1} which is the C-H absorption region of methoxy group, also supported by the presence of a peak at wavenumber 1299 cm^{-1} which is the C-O ether (Nandiyanto et al., 2019). Then the peak 1666 cm^{-1} region indicates the presence of the C=O carbonyl functional group and the peak in the 1585 cm^{-1} region indicates the presence of the C=N group (Daoui et al., 2023), and the last an aromatic C-H peak was also detected at 3057 cm^{-1}.

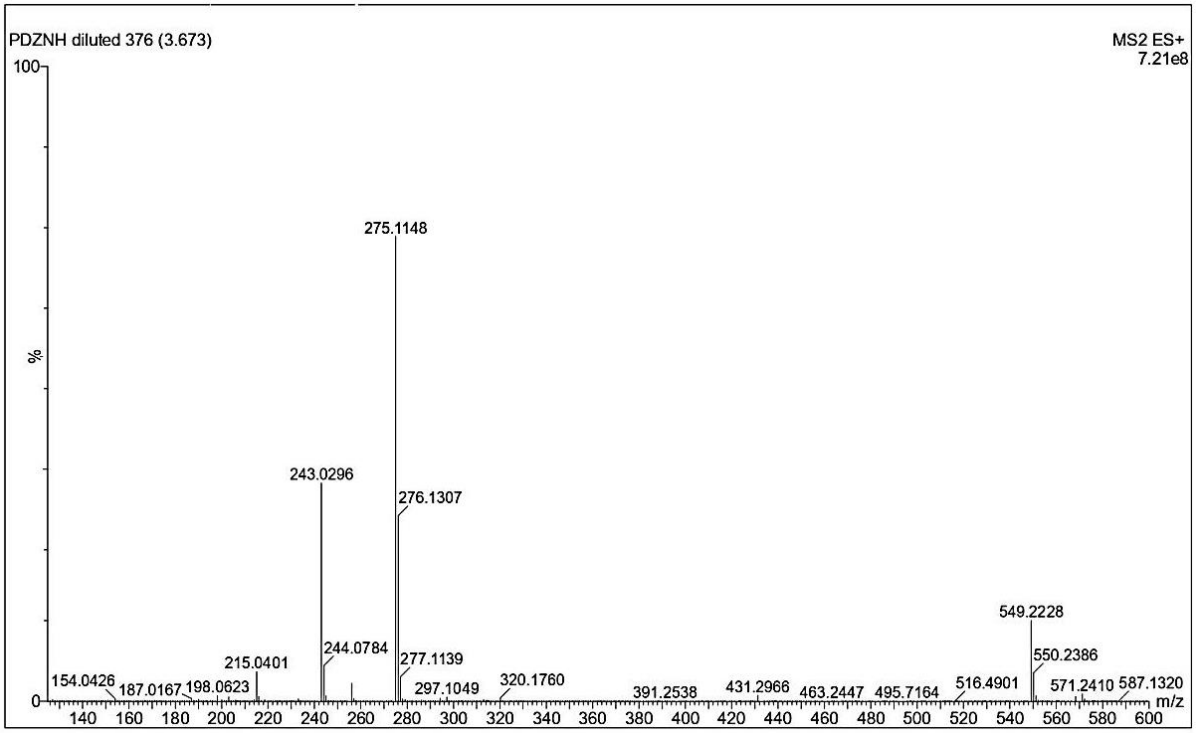

Figure 2. Mass spectrum of compound **(3).**

Furthermore, analysis is carried out using mass spectrometry to determine the molecular weight of the target compound. In mass spectrometry analysis, the sample analysis process involves ionisation of the sample into gaseous form with or without fragmentation, then analysed based on the mass to charge ratio (m/z) and the relative abundance of the ions. The ionisation process can be represented as molecular ions or fragment ions in Figure 2 there is a peak with the highest abundance at m/z 275.11 which is M+ from compound **(3)** (Malik et al., 2015).

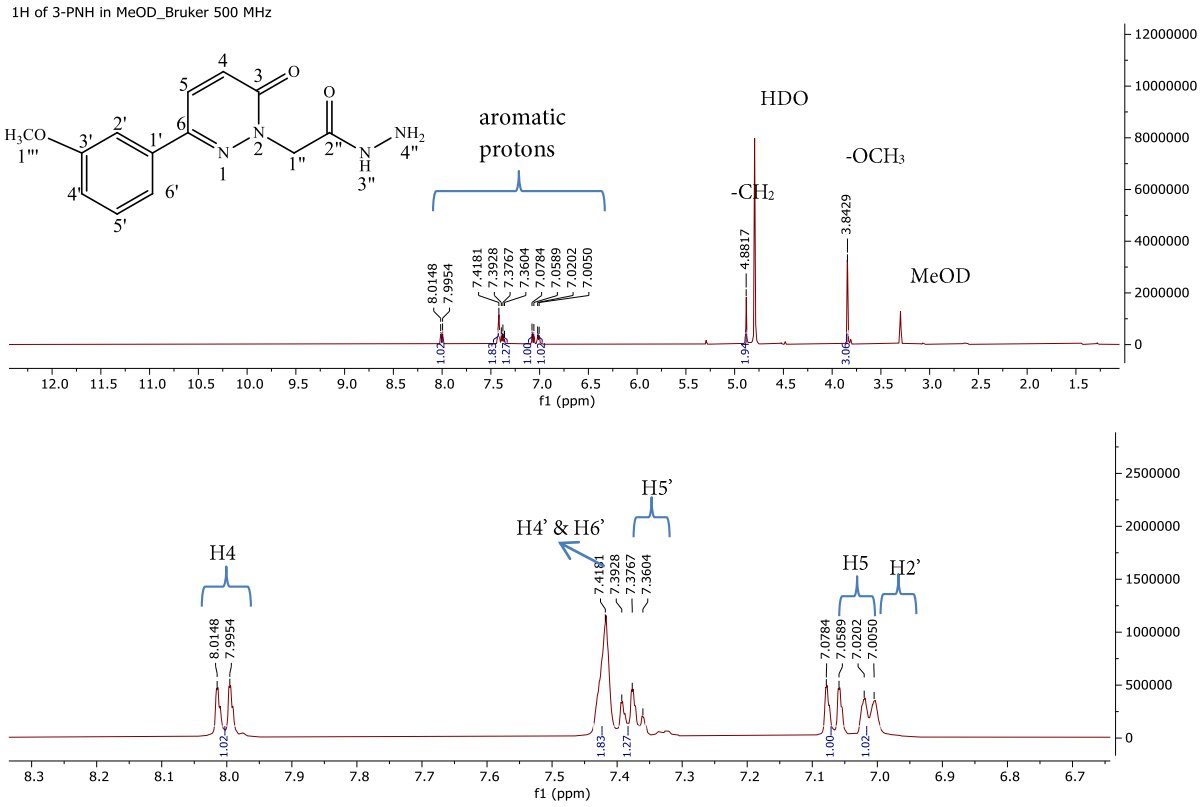

Figure 3. ^{1}H-NMR spectrum of compound **(3).**

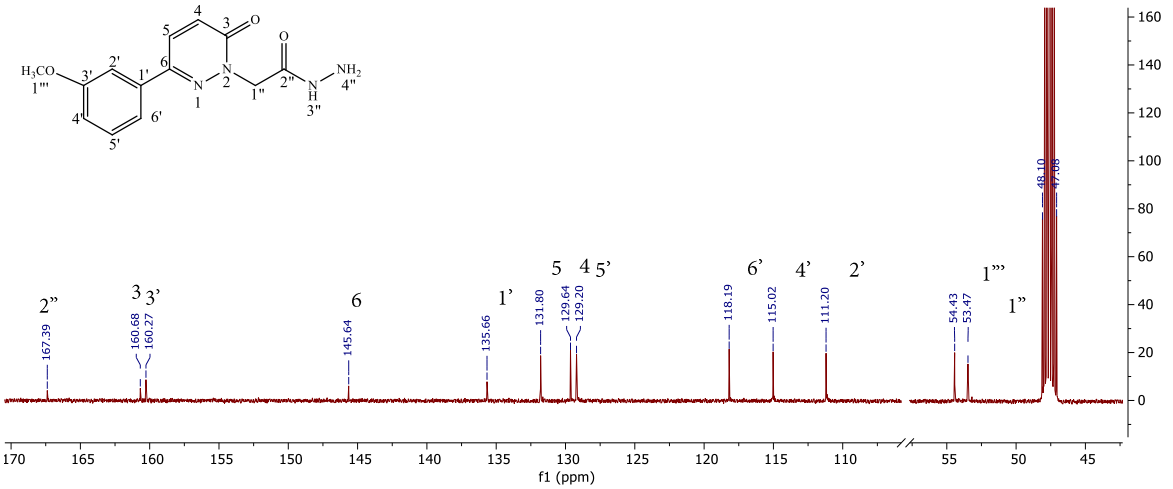

Figure 4. ^{13}C-NMR spectrum of compound **(3).**

The ^{1}H NMR spectrum of compound (3) can be seen in Figure 3, and its interpretation is summarised in Table 1. Methylene protons are characterised by the presence of a singlet signal at δH 4.88 ppm. Then at δH 3.84 there is a peak that indicates the proton of the methoxy group (-OCH_3). In addition, there are three peaks at δH 8.01-7.00 with a total number of integrations of five which indicate aromatic protons (-CH=). The spectrum of 13C NMR (Figure 4) measurement results shows that compound **(3)**. It can be seen that a C carbonyl characterised by the presence of peaks pointing upwards at δC 167.39 and 160.68 ppm which indicates the peak of the C=O. The methylene peak appears at δC 53.47 ppm, while the methoxy peak appears at δC 54.43 ppm.

Table 1. Interpretation of the ^{1}H and ^{13}C-NMR spectra of compound (3)

	Position	δ (ppm) (Multiplicity, J, H)	δ_C (ppm)
	1	-	-
	2	-	-
	3	-	160.68
	4	8.0148-7.9954 (d, J= 9.7 Hz, 1H)	129.64
	5	7.0784-7.0589 (d, J=9.7 Hz, 1H)	131.80
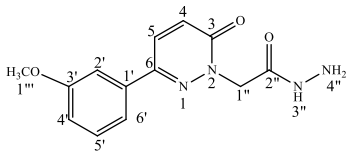	6	-	145.64
	1’	-	135.66
	2’	7.02-7.00 (d, J= 7.6 Hz ,1H)	111.20
	3’	-	160.27
	4’	7.4181 (s, 2H)	115.02
	5’	7.3928-7.3604 (t, J= 8.05, 1H)	129.20
	6’	7.4181 (s, 2H)	118.19
	1”	4.8817 (s, 2H)	53.47
	2”	-	167.39
	3”	-	-
	4”	-	-
	1”’	3.8429 (s, 3H)	54.43

The analysis of IR, MS, ^{1}H NMR, and ^{13}C NMR spectra of compound **(3)** showed the presence of peaks representing certain functional groups that are characteristic of the compound. Therefore, the

structure of compound **(3)** can be concluded to be in accordance with the structure of the target compound.

3.2. Molecular docking studies

A molecular docking study was conducted to determine the potential interaction between the target compound and ER-α, which is one of the target receptors for breast cancer treatment (Ikhtiarudin et al., 2022). The receptor with PDB code 3ERT was chosen as the docking target because it binds 4-hydroxytamoxifen (4-OHT). Tamoxifen is a drug commonly used in breast cancer treatment that acts as an antiestrogenetic. This drug works by blocking the binding of a coactivator to the receptor so as to inhibit the signal pathways responsible for breast cancer cell proliferation (Shiau et al., 1998).

Before docking the target compound with the 3ERT receptor, first validate the docking method by re-docking the 3ERT receptor protein with its natural ligand, 4-OHT (Bhojwani & Joshi, 2017). The redocking results showed a good overlay between the 3ERT receptor complex obtained from RSCB and the redocked 3ERT receptor complex. This indicates that the ligand is bound to the same active side position in both complexes. One of the parameters of docking results is the value of RMSD (Root Mean Square Deviation), a docking method is said to be valid if the value of RMSD < 2Å (Amrulloh et al., 2023). The docking result between 3ERT protein and its natural ligand showed RMSD value of 1.70 Å and binding free energy value of -11.056 kcal/mol, so the docking method is valid. In addition, seen in Figure 5, there is a good positional similarity between the natural ligand 3ERT complex obtained from RCSB with the natural ligand 3ERT complex redocking results. This shows the active side selected in the docking method is in accordance with the position of the natural ligand bound.

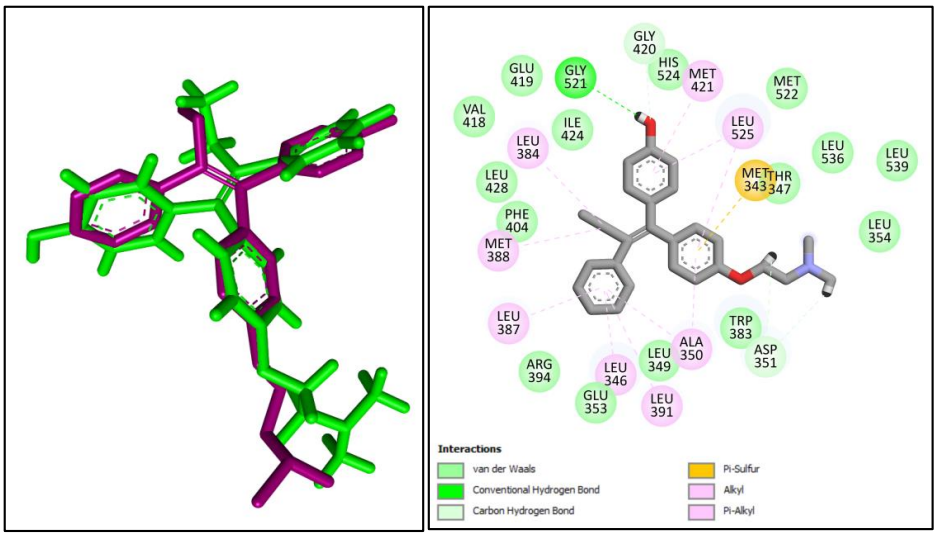

Figure 5. Overlay of redocking binding poses between innate natural ligands (purple) with redocking natural ligands (green).

The docking result between 3ERT protein and its natural ligand showed RMSD value of 1.70 Å and binding free energy value of -11.056 kcal/mol, so the docking method is valid. In addition, seen in Figure 5 and Table 2, there is a good positional similarity between the natural ligand 3ERT complex obtained from RCSB with the natural ligand 3ERT complex redocking results. This shows the active side selected in the docking method is in accordance with the position of the natural ligand bound.

Table 2. Docking result on 3ERT receptor.

Compounds	*ΔS* (kcal/mol)	RMSD	Interaction	
			Hydrogen Bond	Other Interactions

4-OHT (native ligan)	-11.056	1.70	Gly521	Gly420, His524, Met421, Leu525, Met522, Met343, Thr347, Leu536, Leu539, Leu354, Asp351, Trp383, Ala350, Leu349, Leu391, Leu346, Glu353, Arg394, Leu387, Met388, Phe404, Leu428, Phe404, Leu428, Leu384, Ile424, Val418, Glu419.
Tamoxifen	-10.153	1.71	-	Arg394, Glu353, Leu349, Leu391, Ala350, Met343, Leu387, Thr347, Asp351, Lys529, Met528, Trp383, Leu525, Met522, Gly521, His524, Met421, Gly420, Glu419, Ile424, Leu428, Met388, leu384, Phe 404, leu346
(3)	-7.936	0.98	Glu353, Leu387	Met388, Arg394, Leu394, Leu391, Ala350, Phe404, Thr347, Leu346, Leu525, Met343, Glu419, His524, Gly420, Ile424, Gly521, Met421, Leu384.

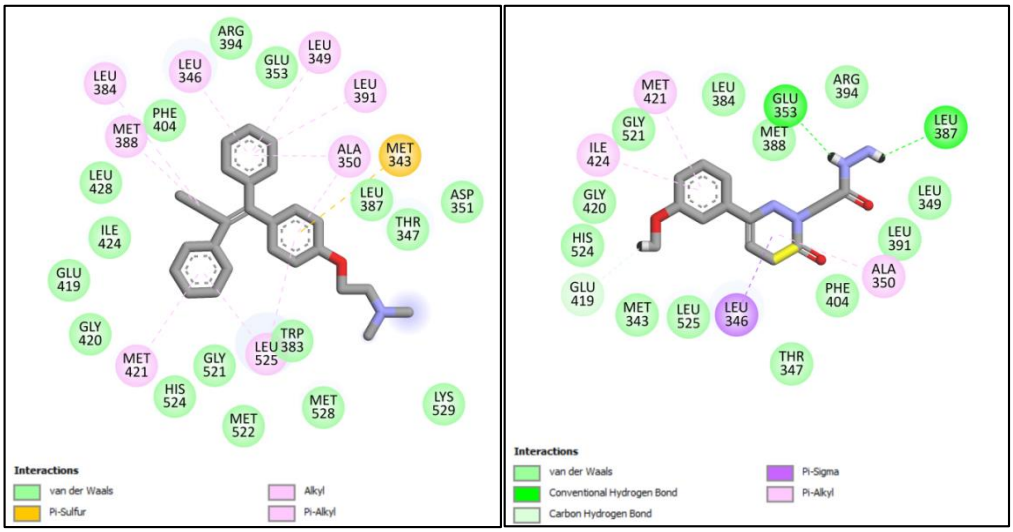

Figure 6. Visualization of ligand interaction with 3ERT receptor a. Tamoxifen, b. compound **(3).**

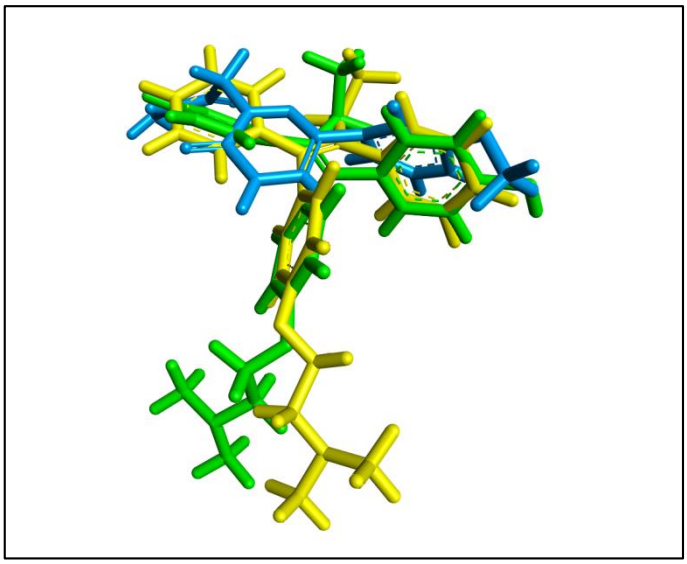

Figure 7. Overlay of binding poses between 4-OHT redocking (green), tamoxifen (yellow) and 3-PNH compound (blue).

Visualization of the interaction of compound **(3)** and tamoxifen compounds with 3ERT protein docking results can be seen in Figure 6. Compound **(3)** is seen to have two hydrogen bonds, namely with amino acids Glu353 and Leu387, while tamoxifen as a positive control does not form hydrogen bonds with amino acids on the active side of the protein. Hydrogen bonds regulate the stability of the host-guest complexes formed (Vaidyanathan et al., 2023). Ligands that have many conventional hydrogen bonds show strong affinity to ER-α (Masand et al., 2024).

The compound **(3)** has hydrogen bonds that tamoxifen does not have. So that the affinity of the compound **(3)** complex with the 3ERT receptor is better. However, the docking results of compound **(3)** with ER-α protein showed greater energy than tamoxifen, namely -7.93 kCal/mol, which indicates low binding affinity. Therefore, the binding affinity of tamoxifen is better than that of compound **(3)**. Overlaying the binding poses of the natural ligand, tamoxifen and compound **(3)** was done to compare the position of the ligand on the active site of ER-α protein. Based on Figure 7. it can be observed that compound **(3)** has a similar binding pose to tamoxifen and natural ligand.

3.3. ADMET profiles

The physicochemical properties of compound **(3)** were analyzed based on Lipinski's rule, which assesses parameters such as molecular weight (MW), the number of hydrogen bond acceptors and donors, as well as logP values that describe the distribution of the compound between n-octanol and water. Based on these criteria, compound **(3)** was predicted to be orally viable and in accordance with Lipinski's rule. Table 3 shows the physicochemical and pharmacokinetic prediction data of compound **(3).**

Table 3. ADMET profiles of compound **(3).**

ADMET profiles	Ideal values	Values
Lipinski's rule of five		
Molecular Weight	≤ 500	274.28
Hydrogen Bond Donor	≤ 5	3
Hydrogen Bond Acceptor	≤10	7
LogP	≤ 5	0.307
ADME		
Penetration of Blood Brain Barriers (BBB) (cm/s)		+++

Human Intestinal Absorption (HIA)	---
Plasma Protein Binding (PPB) (%)	75.57
Caco2 cell permeability (log cm/s)	-4.727
Volume Distribution (L/Kg)	0.659
Half Time	0.716
Toxicity	
Human hepatotoxicity	++
hERG blockers	---
Drug-induced liver injury (DILI)	+++

Note: for classification endpoints, the predicted probability values are transformed into six symbols: 0-0.1 (---), 0.1-0.3 (--), 0.3-0.5 (-), 0.5-0.7 (+), 0.7-0.9 (++), dan 0.9-1.0 (+++)

Drug absorption was evaluated based on blood-brain barrier (BBB) and human intenstinal absorption (HIA) parameters, which represent the ability to cross the blood-brain barrier and be absorbed by the human digestive system, respectively. Compound **(3)** was classified as having good BBB permeability with empirical values between 0.9-1.0 (Syahri et al., 2023). A low HIA value (0-0.1) indicates low absorption ability in the human gut (Yan et al., 2008) It is likely that compound **(3)** cannot be absorbed efficiently through the gastrointestinal tract. Prediction of drug permeability was done using the Caco-2 cell model which represents human colon adenocarcinoma cells (Frimayanti et al., 2025). Compound **(3)** is thought to have limited permeability in the intestine as indicated by a Caco-2 value of >-5.0 log cm/s. The volume of distribution value of 0.659 L/Kg indicates that compound **(3)** has a fairly balanced distribution between blood and tissue (Smith et al., 2015), which is an indicator of systemic circulation safety and stability. Predicted toxicity of compound **(3)** is seen from the parameters of human hepatotoxicity and DILI which show quite high values that are close to 1. This means that compound **(3)** has the potential to cause liver damage. While the hERG blockers parameter shows a relatively low value (0-0.1), meaning that compound **(3)** most likely does not inhibit the hERG channel so it is safe in terms of cardiotoxicity.

4. Conclusion

Based on the research conducted, the compound 2-(3-(3-methoxyphenyl)-6-oxopyridazine-1(6H)-yl)acetohydrazide (3) was obtained in pure form through three reaction steps with a yield of 48.14%. Evaluation of the compound's activity through molecular docking studies showed that the target compound can form hydrogen bonds with important amino acid residues at the active site of ER-α (PDB 3ERT), such as Glu353 and Leu387. The docking results showed that compound (3) has a lower binding affinity compared with tamoxifen. In addition, although compound (3) exhibits good drug-like properties, it has poor absorption and is therefore less suitable for oral administration.

References

Amrulloh, L. S. W. F., Harmastuti N., Prasetiyo, A., & Herowati, R. (2023). Analysis of Molecular Docking and Dynamics Simulation of Mahogany (Swietenia macrophylla King) Compounds Against the PLpro Enzyme SARS-COV-2. *Jurnal Farmasi Dan Ilmu Kefarmasian Indonesia*, *10*(3), 347–359. https://doi.org/10.20473/jfiki.v10i32023.347-359

Arnold, M., Morgan, E., Rumgay, H., Mafra, A., Singh, D., Laversanne, M., Vignat, J., Gralow, J. R., Cardoso, F., Siesling, S., & Soerjomataram, I. (2022). Current and future burden of breast cancer: Global statistics for 2020 and 2040. *Breast*, *66*. https://doi.org/10.1016/j.breast.2022.08.010

Bhojwani, H. R., & Joshi, U. J. (2017). Pharmacophore and Docking Guided Virtual Screening Study for Discovery of Type I Inhibitors of VEGFR-2 Kinase. *Current Computer-Aided Drug Design*.

https://doi.org/10.2174/1386207319666161214112536
Casale, M. T., Richman, A. R., Elrod, M. J., Garland, R. M., Beaver, M. R., & Tolbert, M. A. (2007). Kinetics of acid-catalyzed aldol condensation reactions of aliphatic aldehydes. *Atmospheric Environment*. https://doi.org/10.1016/j.atmosenv.2007.04.002
Chesney, T. R., Yin, J. X., Rajaee, N., Tricco, A. C., Fyles, A. W., Acuna, S. A., & Scheer, A. S. (2017). Tamoxifen with radiotherapy compared with Tamoxifen alone in elderly women with early-stage breast cancer treated with breast conserving surgery: A systematic review and meta-analysis. In *Radiotherapy and Oncology*. https://doi.org/10.1016/j.radonc.2017.02.019
Clusan, L., Ferrière, F., Flouriot, G., & Pakdel, F. (2023). A Basic Review on Estrogen Receptor Signaling Pathways in Breast Cancer. In *International Journal of Molecular Sciences*. https://doi.org/10.3390/ijms24076834
Daoui, S., Direkel, Ş., Ibrahim, M. M., Tüzün, B., Chelfi, T., Al-Ghorbani, M., Bouatia, M., Karbane, M. El, Doukkali, A., Benchat, N., & Karrouchi, K. (2023). Synthesis, Spectroscopic Characterization, Antibacterial Activity, and Computational Studies of Novel Pyridazinone Derivatives. *Molecules*. https://doi.org/10.3390/molecules28020678
El-Nagar, M. K. S., Shahin, M. I., El-Behairy, M. F., Taher, E. S., El-Badawy, M. F., Sharaky, M., Abou El Ella, D. A., Abouzid, K. A. M., & Adel, M. (2024). Pyridazinone-based derivatives as anticancer agents endowed with anti-microbial activity: molecular design, synthesis, and biological investigation. *RSC Medicinal Chemistry*, *15*, 3529–3557. https://doi.org/10.1039/d4md00481g
Frimayanti, N., Septama, A. W., Teruna, H. Y., & Rahmi, E. P. (2025). In silico investigation of artocarpin, cycloarotcarpin, artocarpanone, and cyanomaclurin for Dengue virus inhibitor DEN2 NS2B/NS3 serine protease. *Journal of Pharmacy & Pharmacognosy Research*, *13*(1), 193–202. https://doi.org/10.56499/jppres24.2052_13.1.193
Gondhowiardjo, S., Christina, N., Ganapati, N. P. D., Hawariy, S., Radityamurti, F., Jayalie, V. F., Octavianus, S., Prawira Putra, A., Sekarutami, S. M., Prajogi, G. B., Giselvania, A., Adham, M., Hamid, A. R. A. H., Widyastuti, E., Prabowo, Y., Aninditha, T., Purwoto, G., Aman, R. A., Siregar, T. P., … Agianda, F. (2021). Five-Year Cancer Epidemiology at the National Referral Hospital: Hospital-Based Cancer Registry Data in Indonesia. *JCO Global Oncology*, *7*. https://doi.org/10.1200/go.20.00155
Ikhtiarudin, I., Dona, R., Frimayanti, N., Utami, R., Susianti, N., & Septama, A. W. (2022). Sintesis, Karakterisasi Struktur, dan Kajian Molecular Docking Senyawa Turunan 4'-Metoksi Flavonol sebagai Antagonis Reseptor Estrogen Alpha (ER-a) pada Kanker Payudara. *Jurnal Riset Kimia*, *13*(2), 236–249. https://doi.org/10.25077/jrk.v13i2.553
Malik, A. K., Kumar, R., & Heena. (2015). Spectroscopy: Types. In *Encyclopedia of Food and Health* (1st ed.). Elsevier Ltd. https://doi.org/10.1016/B978-0-12-384947-2.00643-7
Masand, V. H., Al-Hussain, S. A., Alzahrani, A. Y., Al-Mutairi, A. A., Hussien, R. A., Samad, A., & Zaki, M. E. A. (2024). Estrogen Receptor Alpha Binders for Hormone-Dependent Forms of Breast Cancer: e-QSAR and Molecular Docking Supported by X-ray Resolved Structures. *ACS Omega*, *9*(14), 16759–16774. https://doi.org/10.1021/acsomega.4c00906
Meister, K., Paananen, A., & Bakker, H. J. (2017). Identification of the response of protein N-H vibrations in vibrational sum-frequency generation spectroscopy of aqueous protein films. *Physical Chemistry Chemical Physics*. https://doi.org/10.1039/c6cp08325k
Merde, İ. B., Önel, G. T., Akkoç, S., Karaköy, Z., & Türkmenoğlu, B. (2023). Focusing on New Piperazinyl-methyl-3(2H)pyridazinone Based Derivatives: Design, Synthesis, Anticancer Activity and Computational Studies. *ChemistrySelect*, *8*(25). https://doi.org/10.1002/slct.202300910
Mirzaei, M., Sheikholeslami, S. A., Jalili, A., Bereimipour, A., Sharbati, S., Kaveh, V., & Salari, S. (2022). Investigating the molecular mechanisms of Tamoxifen on the EMT pathway among patients with

breast cancer. *Journal of Medicine and Life*. https://doi.org/10.25122/jml-2022-0085

Moo, T. A., Sanford, R., Dang, C., & Morrow, M. (2018). Overview of Breast Cancer Therapy. In *PET Clinics*. https://doi.org/10.1016/j.cpet.2018.02.006

Nandiyanto, A. B. D., Oktiani, R., & Ragadhita, R. (2019). How to read and interpret ftir spectroscope of organic material. *Indonesian Journal of Science and Technology*. https://doi.org/10.17509/ijost.v4i1.15806

Ong, S. K., Haruyama, R., Yip, C. H., Ngan, T. T., Li, J., Lai, D., Zhang, Y., Yi, S., Shankar, A., Suzanna, E., Jung, S. Y., Ho, P. J., Yusuf, A., Nessa, A., Jung, K. W., Fernando, E., Baral, S., Bagherian, M., Pradhan, P., … Anderson, B. O. (2024). Feasibility of monitoring Global Breast Cancer Initiative Framework key performance indicators in 21 Asian National Cancer Centers Alliance member countries. *EClinicalMedicine*, *67*. https://doi.org/10.1016/j.eclinm.2023.102365

Oskoueian, A., Amin Matori, K., Bayat, S., Oskoueian, E., Ostovan, F., & Toozandehjani, M. (2018). Fabrication, Characterization, and Functionalization of Single-Walled Carbon Nanotube Conjugated with Tamoxifen and Its Anticancer Potential against Human Breast Cancer Cells. *Journal of Nanomaterials*, *2018*. https://doi.org/10.1155/2018/8417016

Qin, J., Zhu, M., Zhu, H., Zhang, L., Fu, Y., Liu, J., Wang, Z., & OuYang, G. (2020). Synthesis and antitumor activity of novel pyridazinone derivatives containing 1,3,4-thiadiazole moiety. *Phosphorus, Sulfur and Silicon and the Related Elements*, *195*(7). https://doi.org/10.1080/10426507.2020.1737062

Shiau, A. K., Barstad, D., Loria, P. M., Cheng, L., Kushner, P. J., Agard, D. A., & Greene, G. L. (1998). The structural basis of estrogen receptor/coactivator recognition and the antagonism of this interaction by tamoxifen. *Cell*. https://doi.org/10.1016/S0092-8674(00)81717-1

Smith, D. A., Beaumont, K., Maurer, T. S., & Di, L. (2015). Volume of Distribution in Drug Design. *Journal of Medicinal Chemistry*. https://doi.org/10.1021/acs.jmedchem.5b00201

Syahri, J., Hilma, R., Nurlaili, Sari, M. K., Frimayanti, N., Ali, A. H., & Latip, J. (2023). Synthesis, Antimalarial Activities of Secondary Amine-Substituted Eugenol Compounds against Plasmodium falciparum and in silico Molecular Docking Analysis. *Sains Malaysiana*. https://doi.org/10.17576/jsm-2023-5212-09

Vaidyanathan, R., Murugan Sreedevi, S., Ravichandran, K., Vinod, S. M., Hari Krishnan, Y., Babu, L. K., Parthiban, P. S., Basker, L., Perumal, T., Rajaraman, V., Arumugam, G., Rajendran, K., & Mahalingam, V. (2023). Molecular docking approach on the binding stability of derivatives of phenolic acids (DPAs) with Human Serum Albumin (HSA): Hydrogen-bonding versus hydrophobic interactions or combined influences? *JCIS Open*. https://doi.org/10.1016/j.jciso.2023.100096

Xu, J., Meng, Y. Z., Wang, S. J., & Hay, A. S. (2006). Synthesis and characterization of poly(arylene ether)s containing 6-(4-hydroxyphenyl)pyridazin-3(2H)-one or 6-(4-hydroxyphenyl)pyridazine moieties. *Journal of Polymer Science, Part A: Polymer Chemistry*, *44*(10). https://doi.org/10.1002/pola.21441

Yan, A., Wang, Z., & Cai, Z. (2008). Prediction of human intestinal absorption by GA feature selection and support vector machine regression. *International Journal of Molecular Sciences*. https://doi.org/10.3390/ijms9101961

Yuliastuti, F., Andayani, T. M., Endarti, D., & Kristina, S. A. (2023). Breast, cervical, and lung cancer: A comparison of real healthcare costs and INA-CBGs rates in the era of national health insurance. *Pharmacy Practice*, *21*(1). https://doi.org/10.18549/PharmPract.2023.1.2768